Journal of Inorganic Biochemistry 199 (2019) 110754

Contents lists available at ScienceDirect

Journal of Inorganic Biochemistry

journal homepage: www.elsevier.com/locate/jinorgbio

Novel anticancer Pd^{II} complexes: The effect of the conjugation of transferrin binding peptide and the nature of halogen coordinated on antitumor activity

C.M. Teles[a], L.C. Lammoglia[b], M.A. Juliano[c], A.L.T.G. Ruiz[b], T.Z. Candido[d], J.E. de Carvalho[b], C.S.P. Lima[d], C. Abbehausen[a,*]

[a] Institute of Chemistry, University of Campinas – UNICAMP, PO Box 6154, 13083-970 Campinas, SP, Brazil
[b] Faculty of Pharmaceutical Sciences, University of Campinas, UNICAMP, 13083-871 Campinas, SP, Brazil
[c] Universidade Federal de São Paulo, Escola Paulista de Medicina, UNIFESP, 04063-062 São Paulo, SP, Brazil
[d] Faculty of Medical Sciences, University of Campinas, UNICAMP, 13083-970 Campinas, SP, Brazil

ARTICLE INFO

Keywords:
Palladium
Antitumor activity
Selectivity

ABSTRACT

A series of Pd^{II} complexes with bis-(2-pyridylmethyl)glycine as a ligand of formula [PdX(bis-(2-pyridylmethyl) glycine)] where X = Cl, Br, I were prepared and the effect of the halogen nature in the antitumor activity of eight tumorigenic and one non-tumorigenic cell line was evaluated. The chloride derivative was further functionalized with a transferrin receptor binding peptide, generating the first Pd^{II} based metallopeptide. Its antitumor activity was also evaluated. However, among all the complexes, the chloride and iodine parent compounds showed the lowest GI_{50} values in the panel evaluated, and lowest GI_{50} than cisplatin in several cell lines. In contrast, the bromine derivative showed higher values of GI_{50} than chloride and iodine (around 30 – 50 μM). The same trend was observed for the bovine serum albumin binding constant with higher values for iodine, chlorine, and bromine in this order. In aqueous solution, the chloride is exchanged by water while the bromine and iodine are not. DNA was evaluated as a target and showed no significative interaction for all the compounds. The results suggest sulfur-rich proteins and not DNA as a target. This report represents the first Pd^{II} metallopeptide reported, its evaluation in solution and antitumor activity. This work opens the possibilities for further functionalization of Pd^{II} complexes and the importance of the halogen coordination in the design of novel metallodrugs.

1. Introduction

Metal complexes are chemically and structurally very versatile. The nature of ligands chosen can provide a rich diversity of chemical, electronic and kinetic properties. This versatile chemistry allows the design of compounds that can target biomolecules and act in therapeutics and diagnostics [1,2]. However, it is also recognized the poor cell permeability of metal-based compounds and also their lack of selective delivery to the sites of disease [3–5]. Among multiple strategies, conjugation of metal complexes to peptides is a promising one to enhance their uptake properties, site-selective delivery and selective internalization [5]. The pioneering work of Lippard and co-workers on the functionalization of Pt^{IV} complexes with peptides, rendering selective recognition to malignant cells expressing $\alpha_v\beta_3$ and $\alpha_v\beta_5$ integrins, is an important example [6]. Several reports on the conjugation of cell-penetrating peptides to Ru^{II}, Os^{II}, Re^{I}, and Pt^{IV} showed enhancement of cell uptake [7–10]. Although this enhancement is not usually expressed as an increase of *in vitro* activity when compared to the parent compound, the efficiency is increased [11,12].

The transferrin receptor (TfR) is a transmembrane protein responsible for the iron homeostasis carried by transferrin (Tf) [13–16]. The transferrin receptor is an attractive target for anticancer compounds as it is upregulated in the surface of cancer cells and it efficiently internalizes transferrin and other peptides, called TfR binding peptides [17–19]. The conjugation of anticancer drugs to Tf or TfR binding peptides is a promising strategy to offset the side effects or circumvent the resistance [20,21]. The highly used anticancer drug doxorubicin was conjugated to Tf yielding a compound 3 and 10 fold more cytotoxic than doxorubicin alone in sensitive and resistant cell lines respectively [22]. Cisplatin chemically conjugated to the iron-binding sites of Tf inhibits the growth of human adenocarcinoma *in vitro* and *in vivo* [23]. The peptide HAIYPHRH, first screened by phage display on cells expressing human TfR showed a high affinity for this receptor (Kd ~ 10^9) and a different binding site from that of Tf [24]. The different binding site is advantageous because the endogenous Tf does not inhibit the uptake of the peptide [25].

* Corresponding author.
E-mail address: camilla@unicamp.br (C. Abbehausen).

https://doi.org/10.1016/j.jinorgbio.2019.110754
Received 26 February 2019; Received in revised form 14 June 2019; Accepted 23 June 2019
Available online 27 June 2019
0162-0134/

Although peptide conjugation is an interesting strategy, their preparation is challenging because of the chemical functionality of peptides and the lability of metal complexes. Solid phase peptide synthesis has been the most prominent method to obtain conjugates [26–28]. Ligands as tris-(2-pyridylmethyl)amine (tpa), *N*,*N*-bis(2-picolyl)amine (bpa) or 2,2'-dipicolylamine (dpa) are very useful as they can be anchored to the peptide bound in the resin, cleaved and unprotected in concentrated acid and, after purification, reacted with metal salts [29,30].

The interest in the study of anticancer activity of Pd^{II} complexes comes from the electronic and structural similarities to the Pt^{II} complexes. However, their fast kinetics on ligand substitution reactions turns the Pd^{II} complexes inactive and highly toxic [31,32]. Coordination of chelating, macrocyclic ligands, sterically hindered ligands in *trans* geometry, and ligands with strong π receptor abilities demonstrated to circumvent the lower activity and the intrinsic toxicity of Pd^{II} complexes, as demonstrated by early *in vivo* studies [33–38]. Although some Pd^{II} complexes present higher activity than their respective Pt^{II} derivatives or cisplatin they did not present the demanding characteristics to be a successful antitumor agent in the clinic. However, the results have been encouraging researchers for the design of new Pd^{II} anticancer drugs [31,39–41]. No reports of Pd^{II} complexes conjugated to peptides or other biomolecules are found up to date. Furthermore, we have investigated how the nature of the halogen coordinated affects antitumor activity. Previous reports have demonstrated the coordination of iodine to metals can considerably affect antitumor activity. Firstly, it was found in that replacement of the chloride ligands to give the diiodide complex cis-$[PtI_2(NH_3)_2]$ completely vanished the activity of the complex [42]. Since that report, there have been a few studies of the effects of Cl–I substitutions on the activity of transition metal complexes, although active trans Pt^{II} diiodide complexes bearing isopropylamine, dimethylamine or methylamine ligands have been reported [43]. For Ru^{II} and Os^{II} arene complexes the substitution Cl^- to I^- improved activity and selectivity [44].

In this work, we report for the first time the coordination of Pd^{II} to bis-(2-pyridylmethyl)glycine (bpg). The fourth coordination site was completed by halogens Cl, Br and I. The chloride derivative was conjugated to a transferrin receptor binding peptide (TrfR-pep) as demonstrated in Fig. 1. The antitumor activity and the interaction with bovine serum albumin (BSA) and DNA were investigated. It was found the halogen nature can change significantly the interaction with biomolecules and consequently changing the antitumor activity. The conjugation turned the complex insoluble enough to affect its antitumor activity.

2. Experimental

2.1. Materials and equipment

Ligand bpg was synthesized as previously described [45]. All chemicals used in this work were reagent grade and used without further purification. The metal complex $K_2[PdCl_4]$ was acquired from Sigma Aldrich. The elemental analyses (CHNS) were determined using a Perkin-Elmer 2400 CHNS/O elemental analyzer. The electrospray ionization mass spectra (ESI-MS) in the positive and negative mode were recorded with a Waters TQD Quattro Micro API or a Waters Xevo QTof MS equipment. Infrared (IR) spectra were obtained by attenuated reflectance in an Agilent Cary 630 FTIR spectrophotometer in the wavenumber range of 600 and 4000 cm^{-1}. The electronic spectra were recorded with a Hewlett Packard 8453 instrument with a coupled temperature controller Peltier unit. Solution ^1H and ^{13}C were acquired on a Bruker Avance III 400 and 500 MHz multinuclear spectrometer, using tetramethylsilane as the reference for ^1H and ^{13}C NMR. Circular dichroism spectra were obtained in a Jasco J720 spectropolarimeter. Fluorescence experiments were conducted with an Agilent Cary Eclipse fluorescence spectrophotometer with a temperature controller Peltier unit and magnetic stirring, using a cuvette with 10 mm optical path and volume of 3 mL. Single crystal data collection was performed with a Bruker Apex II CCD diffractometer with graphite monochromator Mo Kα (K = 0.71703 Å) radiation. Accurate unit cell dimensions and orientation matrices were determined by the least-squares refinement of the reflections obtained by ϴ-χ scans. The data were indexed and scaled with the ApexII Suite [APEX2 v2014.1-1 (Bruker AXS), SAINT V8.34A (Bruker AXS Inc., 2013)]. Bruker Saint and Bruker Sadabs were used to integrate and for scaling of data, respectively. The structure was solved using the software OLEX2 and the refinement extended using the program SHELXT [46,47]. The structure was refined using Direct Methods implemented in the SHELXL by applying a full-matrix least-squares technique on F2 [48]. All non-hydrogen atoms were refined anisotropically. The hydrogen atoms in the compound were added to the structure in idealized positions and further refined according to the riding model; molecular graphics. OLEX2 and Mercury 3.9 software was used to prepare material for publication [47].

2.2. Synthesis of the complex [PdCl(bpg)]

The complex [PdCl(bpg)] was synthesized by adding 1 mL of aqueous solution containing 0.33 mmol of the ligand bpg to 1 mL of aqueous $K_2[PdCl_4]$ (100 mg, 0.31 mmol). Immediately, the red solution

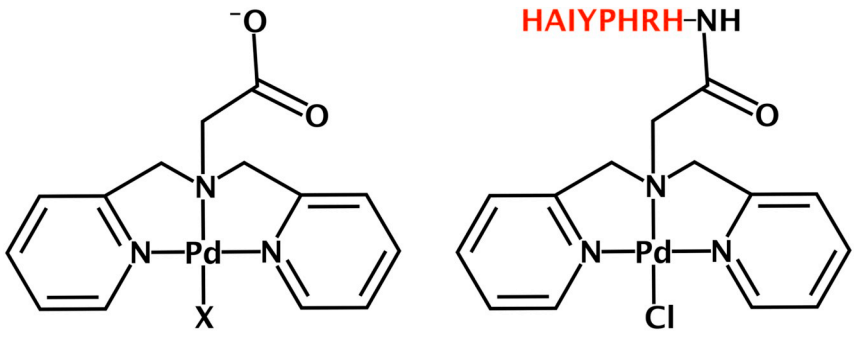

Figure 1. The molecular formula of Pd^{II} complexes and conjugation represented by peptide sequence (red). (For interpretation of the references to colour in this figure legend, the reader is referred to the web version of this article.)

turned yellow and after 30 min stirring at RT a yellow solid precipitated. The solid was filtered and washed with cold water. The complex was obtained as a yellow powder. Single crystals were obtained by slowly evaporation of water. Yield: 51% Anal. calc. for $[C_{14}H_{14}ClN_3O_2Pd].(H_2O)$: C 40.41; H 3.88; N 10.10; Found: C 40.40; H 4.03; N 9.96. ^{1}H NMR (500 MHz, DMSO-d_6): δ(ppm) 8.55 (dd, *Jm = 0.8* Hz, *Jo = 5.8* Hz, 2H); 8.18 (td, *Jm = 1.5* Hz, *Jo = 7.8* Hz, 2H); 7.77 (d, *J = 7.8* Hz, 2H); 7.62 (d, *J = 6.7* Hz,2H); 5.55 (d, *J = 16.2* Hz, 2H); 5.83(d, *J = 16.2* Hz, 2H); 4.22 (s, 2H). ^{13}C NMR (125 MHz, DMSO): δ (ppm) 174.1; 158.5; 149.0; 137.7; 123.3; 123.1; 60.4; 58.9. ESI-MS (*m/z*): Monoisotopic mass: 397.9864 $[PdCl(bpg)]^+$ (calc. 397.9890).

2.3. Synthesis of the complexes [PdX(bpg)] where X = Br and I

Complex [PdBr(bpg)] was synthesized by chloride exchange of complex [PdCl(bpg)] adding $AgNO_3$ (41.6 mg, 0.24 mmol) to a water suspension of [PdCl(bpg)] (100 mg, 0.25 mmol) and stirring at dark for 24 h. After reaction time, the AgCl formed was removed by filtration through Celite. To the yellow solution was added 5 times equivalent of NaBr (127.5 mg, 1.25 mmol) and after 16 h yellow crystals precipitated. Yield: 43% Anal. calc. for $C_{14}H_{14}BrN_3O_2Pd{\cdot}5H_2O$: C 31.57; H 4.54; N 7.89; Found: C 31.33; H 4.49; N 7.62. ^{1}H NMR: (400 MHz, D_2O): δ(ppm) 8.79 (s, 2H); 8.08 (t, *J = 7.6* Hz, 2H); 7.62 (d, *J = 7.8* Hz, 2H); 7.49 (t, *J = 6.1* Hz, 2H); 5.38 (d, *J = 16.2* Hz, 2H); 4.92 (d, *J = 16.0* Hz, 2H); 3.84 (s, 2H). ESI-MS (*m/z*): Monoisotopic mass: 442.0268 $[PdBr(bpg)]^+$ (calc. 441.9383).

Complex [PdI(bpg)] was synthesized in analogous way to [PdBr (bpg)] but with addition of KI (207.5 mg, 1.25 mmol) in the place of NaBr. Complex [PdI(bpg)] was obtained as an orange solid. Yield: 65% Anal. calc. for $(C_{14}H_{14}IKN_3O_2Pd)I{\cdot}2H_2O$: C 24.31; H 2.62; N 6.08; Found: C 24.47; H 2.86; N 6.03. ^{1}H NMR: (400 MHz,D_2O): δ(ppm) 9.25 (d, *J = 5.6 Hz*, 2H); 8.08 (t, *J = 7.28* Hz, 2H); 7.66 (d, *J = 7.8* Hz, 2H); 7.45 (t, *J = 6.6* Hz, 2H); 5.53 (d, *J = 15.9* Hz, 2H); 4.92 (d, *J = 15.9* Hz, 2H); 3.82 (s, 2H). ESI-MS (*m/z*): Monoisotopic mass: 490.0091 $[PdI(bpg)]^+$ (calc. 489.9250).

2.4. pKa determination by potentiometric titration

The pKa was determined by potentiometric titration. The burette was calibrated and the NaOH solution was standardized by titration with potassium acid phthalate using phenolphthalein as an indicator. The concentration determined was 8.6 mmol. Three solutions of [PdCl (bpg)] (0.342 mM, 0.468 mM and 0.645 mM) were titrated with NaOH 8.6 mM and the pH measured using a glass electrode and registered each 50 μL addition. The three curves of pH × volume of NaOH were plotted using Origin 9.0 and the pKa was determined using the CurTiPot 3.6.1. [49].

2.5. Halogen hydrolysis by ^{1}H NMR

Three solutions of 600 μL containing 5 mg of the complexes [PdX (bpg)] where X = Cl, Br and I were prepared in D_2O and placed in NMR tubes. The ^{1}H NMR spectra were acquired after 15 min, 1 h and 20 h from the preparation. The tubes were kept in a 25 °C bath for temperature control during the intervals.

2.6. Spectroscopic analysis of DNA interaction with [PdCl(bpg)]

2.6.1. DNA preparation

An appropriate amount of calf-thymus DNA (CT-DNA) was dissolved in deionized water. It was dialyzed for 24 h, using a membrane of 30,000 Da cut-off in a $NaClO_4$ aqueous solution 10.0 mM. The nucleic acid concentration was determined by UV spectrophotometry in properly diluted samples, using the molar absorption coefficient 6600 M^{-1} cm^{-1} at 260 nm [50]. The stock solution concentration used in this work was determined as 1.46 mM. The solution of CT-DNA gave a ratio of UV absorbance at 260 and 280 nm > 1.8, nm greater than indicating that DNA was sufficiently free from protein.

2.6.2. Titration

Titration was performed using two cuvettes. In cuvette **1** (sample cuvette), a stock solution of complex [PdCl(bpg)] was prepared in DMF (9.31 mM) and further diluted in PBS 10 mM NaCl 50 mM pH 7.4 for a final concentration of 20 μM (final DMF volume was 0.215% (*v/v*)). In cuvette **2** (blank cuvette) was added the same volume of pure DMF in PBS 10 mM NaCl 50 mM pH 7.4. Two titrant solutions were used. In cuvette **1**, adequate volumes of stock solution 20 μM of complex with and 1.00 mM CT-DNA in PBS 10 mM NaCl 50 mM pH 7.4 were added to obtain [DNA]/[compound] ratios from 0 to 4.1. In cuvette **2**, was added the same volumes of pure DMF (the same as added in the previous solution) with and 1.00 mM CT-DNA in PBS 10 mM NaCl 50 mM pH 7.4. The spectra were acquired and the absorbance at 265 nm was followed registered.

2.7. Interaction of [PdCl(bpg)] with pGEX-4T1 DNA plasmid

The DNA cleavage activity of the metal complex [PdCl(bpg)] was studied by using agarose gel electrophoresis as described by Shahabadi et al. [39]. Briefly, the plasmid DNA pGEX-4 T1 (100 ng) was dissolved in PBS 10.0 mM pH 7.4 and mixed with serial amounts (50 to 100 μmol) of [PdCl(bpg)] in the same buffer solution containing 5% DMF. The mixtures were incubated at 37 °C for 24 h and then mixed with the Gel Loading Dye Purple (5 μL/sample, BioLabs). Each sample (20 μL) was loaded into 0.8% w/v agarose gel/ethidium bromide. Electrophoresis was undertaken for 90 min at 110 *V* in tris-acetate-EDTA (TAE) buffer. After electrophoresis, the gel was photographed under UV light.

2.8. Synthesis of bpg-TfRpep

Solid phase peptide synthesis with the fluorenyl-9-methoxycarbonyl (Fmoc) methodology strategy was used to obtain the transferrin receptor binding peptide as previously described [51,52]. All the protected amino acids were purchased from Calbiochem-Novabiochem (San Diego, CA, USA) and the synthesis was performed in an automated simultaneous multiple solid phase peptide synthesizer (PSSM 8 system; Shimadzu, Tokio, Japan). The final peptides were deprotected in TFA and purified by semipreparative HPLC using an Econosil C-18 column (10 μm, 22.5 x 250 mm) and a two-solvent system: (A) trifluoroacetic acid (TFA)/H_2O (1:1000) and (B) TFA/acetonitrile (ACN)/H_2O (1:900:100). The column was eluted at a flow rate of 5 mL/min with a 10 (or 30) - 50 (or 60)% gradient of solvent B over 30 or 45 min. Analytical HPLC was performed using a binary HPLC system from Shimadzu with a SPD-10AV Shimadzu UV–vis detector, coupled to an Ultrasphere C-18 column (5 μ, 4.6 × 150 mm) which was eluted with solvent systems A1 (H_3PO_4/H_2O, 1:1000) and B1 (ACN/H2O/H_3PO_4, 900:100:1) at a flow rate of 1.0 mL/min and a 10–80% gradient of B1 over 20 min. The HPLC column eluates were monitored by their absorbance at 220 nm. The molecular weight and purity of synthesized peptides were checked by electron spray LC/MS-2010 (Shimadzu). Subsequently, the ligand bpg was added in DMF solution in the concentration 40 mM (1:10) and kept in a rotatory shaker for 24 h. The product (bpg-TfRpep) was removed from the resin and the amino acid deprotect by addition of concentrated trifluoroacetic acid. After purification, the bpg-TfRpep was characterized by MALDI-MS. *m/z* 1269 calc 1269.

2.9. Synthesis of [PdCl(bpg-TfRpep)]

Purified bpg-TfRpep (15 mg, 12 μmol) was dissolved in deionized water (1 mL). K_2PdCl_4 (4 mg, 12 μmol) was previously dissolved in deionized water (0.5 mL) and the both solutions were mixed. The

Table 1
Structural data from the single-crystal XRD of the $C_{14}H_{15}XN_3O_2Pd{\cdot}3.5(H_2O)$ HO complex, where X can be Cl or Br.

Molecular formula	$C_{14}H_{14}ClN_3O_2Pd{\cdot}3.5(H_2O){\cdot}HO$	$C_{14}H_{14}BrN_3O_2Pd{\cdot}3.5(H_2O){\cdot}HO$
Formula weight ($gmol^{-1}$)	478.19	522.65
λ (Mo, Kα, Å)	0.71073	0.71073
Space Group	C2/c	C2/c
Crystal system	Monoclinic	Monoclinic
a (Å)	28.5040 (18)	28.438 (3)
b (Å)	8.8442 (5)	8.9417 (8)
c (Å)	14.7150 (9)	14.8244 (14)
β (°)	102.157 (1)	100.981 (2)
V ($Å^3$)	3626.4 (4)	3700.6 (6)
Z	8	8
T (K)	150	150
D_x ($mg\,m^{-3}$)	1.752	1.876
F(000)	1936	2080
Reflections collected/unique	36,802/4496	40,856/5645
Data/restraints/parameters	4496/0/337	5645/0/337
R1;*wR2* [$I > 2r$ (I)]	0.020, 0.049	0.017, 0.043
Diff. peak and hole ($e/Å^3$)	0.59, −0.54	0.61, −0.58
Goodness of fit in F^2	1.02	1.03
CCDC deposition number	1871564	1871558

mixture was stirred at 16°C for 24 h, a pale-yellow powder was isolated and characterized. ESI-MS (*m/z*): 685.7621 $[Pd(bpg\text{-}TfRpep)]^{2+}$ (calc. 685.7640), 739.7118 $[Pd(bpg\text{-}TfRpep) + Pd]^{2+}$ (calc. 739.7090), 758.6944 $[Pd(bpg\text{-}TfRpep) + PdCl]^{2+}$ (calc. 758.7048), 775.6879 $[Pd(bpg\text{-}TfRpep) + PdCl_2]^{2+}$ (calc. 775.6851).

2.10. Peptide hydrolysis of [PdCl(bpg-TfRpep)]

To evaluate the solution stability of the peptide in the complex ESI-MS was followed with time after incubation of [PdCl(bpg-TfRpep)] in aqueous solution at 37 °C. The samples were sprayed immediately using a final concentration of ~100 μM. Data were acquired in positive mode. Samples were diluted with a methanol/water (1:1) solution and directly infused at a flow rate of 40 μL/min. The source temperature was maintained at 150 °C throughout. The solution at $t = 0$, 24 and 48 h was monitored by ESI-MS under the same conditions.

2.11. Interaction of [PdX(bpg)] and [PdCl(bpg-TfRpep)] with Bovine Serum Albumin (BSA)

An aqueous solution containing 20 μM BSA was titrated by successive additions of adequate volumes of complex [PdCl(bpg)] solution 7.40 mM, [PdBr(bpg)] solution 7.90 mM, [PdI(bpg)] solution 9.85 mM and [PdCl(bpg-TfRpep)] solution 6.00 mM to final concentrations in the range of 0 to 96 μM. Fluorescence spectra were measured at 298 K in the range of 300 – 450 nm at the excitation wavelength of 280 nm.

2.12. Antiproliferative assay

The antiproliferative activity of [PdX(bpg)], where X = Cl, Br, I and [PdCl(bpg-TfRpep)] was evaluated against nine human tumor cell lines [glioblastoma (U251), prostate cancer (PC-3), breast cancer (MCF7), doxorubicin resistant high-grade ovarian serous adenocarcinoma (NCI-ADR/RES), renal cell carcinoma (786-0), large cell lung carcinoma (NCI-H460), high-grade ovarian serous adenocarcinoma (OVCAR-03), rectosigmoid adenocarcinoma (HT-29), and chronic myelogenous leukemia (K562)] and one non-tumorigenic human keratinocyte (HaCaT). The tumor cell lines were provided by Frederick Cancer Research & Development Center, National Cancer Institute, Frederick, MA, USA, while the non-tumor cell line HaCaT (human keratinocyte) was provided by Dr. Ricardo Della Coletta (University of Campinas, UNICAMP, Brazil).

Stock cultures were grown in 5 mL of Roswell Park Memorial Institute (RPMI) 1640 (Gibco®, USA) supplemented with 5% fetal bovine serum (Gibco®, USA) at 37 °C in 5% CO_2 with a 1% penicillin:streptomycin mixture (Vitrocell®, Brazil; 1000 U/mL:1000 mg/mL) (complete medium). Stock solutions of complexes [PdX(bpg)] and [PdCl(bpg-TfRpep)] were prepared in DMSO (5 mg/mL) followed by serial dilution on complete medium affording the final concentrations of 0.25, 2.5, 25 and 250 μg/mL. Doxorubicin (final concentrations of 0.025, 0.25, 2.5 and 25 μg/mL in complete medium) was used as positive control.

Cells in 96-well plates (100 μL/well, inoculation density: 3.5 to 6×10^4 cell/mL) were exposed to the four concentrations of the complexes and doxorubicin (100 μL/well) in triplicate, for 48 h at 37 °C and 5% of CO_2. Before (T0 plate) and after the sample addition (T1 plates), the cells were fixed with 50% trichloroacetic acid (50 μL/well), and the cell proliferation was determined by the spectrophotometric quantification (540 nm) of the cellular protein content using the sulforhodamine B assay. The GI_{50} values (concentration that inhibits 50% of cell growth) were determined through sigmoidal regression using Origin 8.0 software (OriginLab Corporation, USA) [53–55].

3. Results and discussion

3.1. Single crystal X-ray diffraction characterization of [PdCl(bpg)] and [PdBr(bpg)]

The X-ray structure determination of the complexes [PdCl(bpg)] and [PdBr(bpg)] showed they have a similar coordination geometry. Also, they share the same monoclinic C2/c space group. The detailed cell parameters, as well as the deposit number at Cambridge Crystallographic Data Centre (CCDC), are presented in Table 1. The ORTEP views with atom labeling of [PdCl(bpg)] (Fig. 2a) and [PdBr(bpg)] (Fig. 2b) show the Pd^{II} ion coordinated in distorted square-planar geometry to the three nitrogen atoms present in the tripodal ligand and the fourth coordination site occupied by the halogen atom. The tridentate ligand causes the angle distortion with N1-Pd-N3 and N2-Pd-N3 around 84° for both complexes. These angles were very coherently with $[Pd(dien)L]^{n+}$ and $[Pd(terpy)L]^{n+}$ complexes, where dien = diethylenetriamine and terpy = terpyridine [56–59]. The bond distances are very similar for both complexes, except by the Pd-X which is 2.3057(4) Å for chloride and 2.4257(2) Å for bromide. The carboxylate is uncoordinated and deprotonated and consequently, the units are neutral in both complexes. The carboxylate participates in a net of hydrogen bonds with the water molecules very similar in both complexes. A table with selected bond distances and angles for [PdCl(bpg)] and [PdBr(bpg)] can be found in Table S1. The X-ray structure for

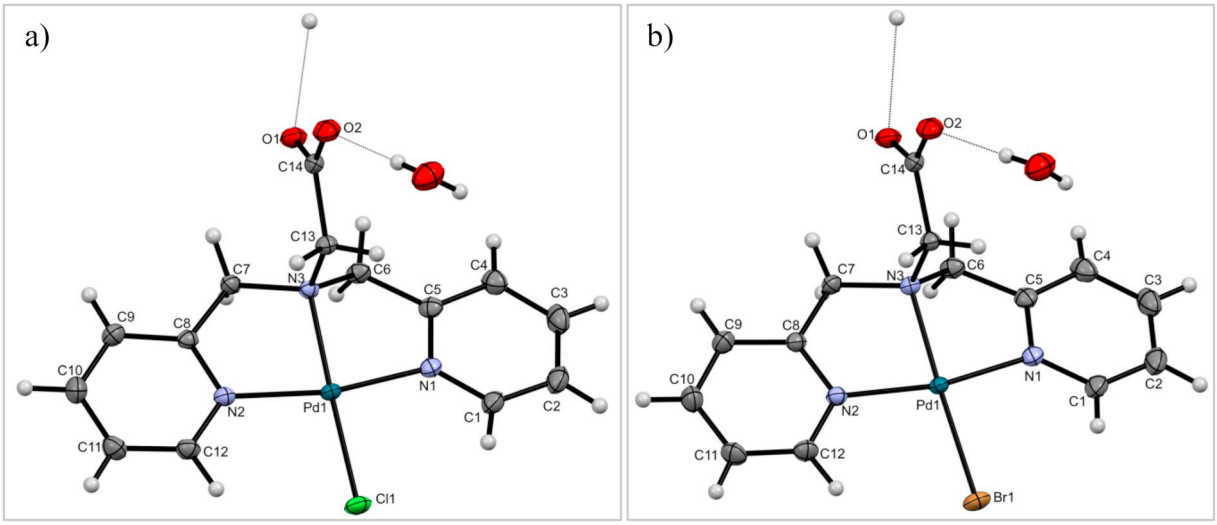

Figure 2. ORTEP view of the crystal structure of a) [PdCl(bpg)] and b) [PdBr(bpg)], assymetric unit, elipsoids represent probability level of 50%.

complex [PdI(bpg)] could not be determined because crystals obtained were not suitable for diffraction, in the CHN analysis we observed a pattern that indicates the presence of KI in the solid, suggesting the structure to be [PdI(bpgK$^+$)]I, where K^+ ion stabilizes free carboxylic group and iodide stabilizes the complex charge.

3.2. Synthesis and spectroscopic characterization in solution

The ^{1}H NMR spectrum of [PdCl(bpg)] in d_6-DMSO is presented in Fig. S1. The main evidence of coordination was the split of the signal of hydrogen 5 in two duplets, assigned as 5 and 5′ which was observed as a singlet in 4.38 ppm in the spectrum of the uncoordinated ligand. The coordination causes the loss of equivalence of hydrogen 5 due to the square planar geometry imposed by the metal. Moreover, the lower field shift of the signals assigned to the hydrogens 6 by 0.67 ppm agrees with the coordination of the amine group. The lower field shift of the hydrogen 1 by 0.10 ppm suggests coordination of the picolyl groups to Pd^{II}. The singlet observed in 3.15 suggests water coordination to the metal due to the halogen exchange. This observation was further confirmed by the signal splitting and secondary signals in the spectrum of [PdCl(bpg)] acquired in D_2O as can be seen in Fig. 3.

The complexes [PdBr(bpg)] and [PdI(bpg)] presented clean spectra in D_2O solution (Fig. 3) compared to [PdCl(bpg)], demonstrating no halogen hydrolysis in these two complexes. Therefore, the characterization of them was performed in aqueous solution. The split of hydrogen 5 is also observed for all the complexes in D_2O, confirming the coordination. The coordination of different halogens affects the chemical shifts, especially of hydrogens 1. In the uncoordinated ligand, hydrogen 1 was found in 8.75 ppm, in [PdBr(bpg)] this signal was shifted to 8.79 ppm and in [PdI(bpg)] it was shifted to 9.25 ppm.

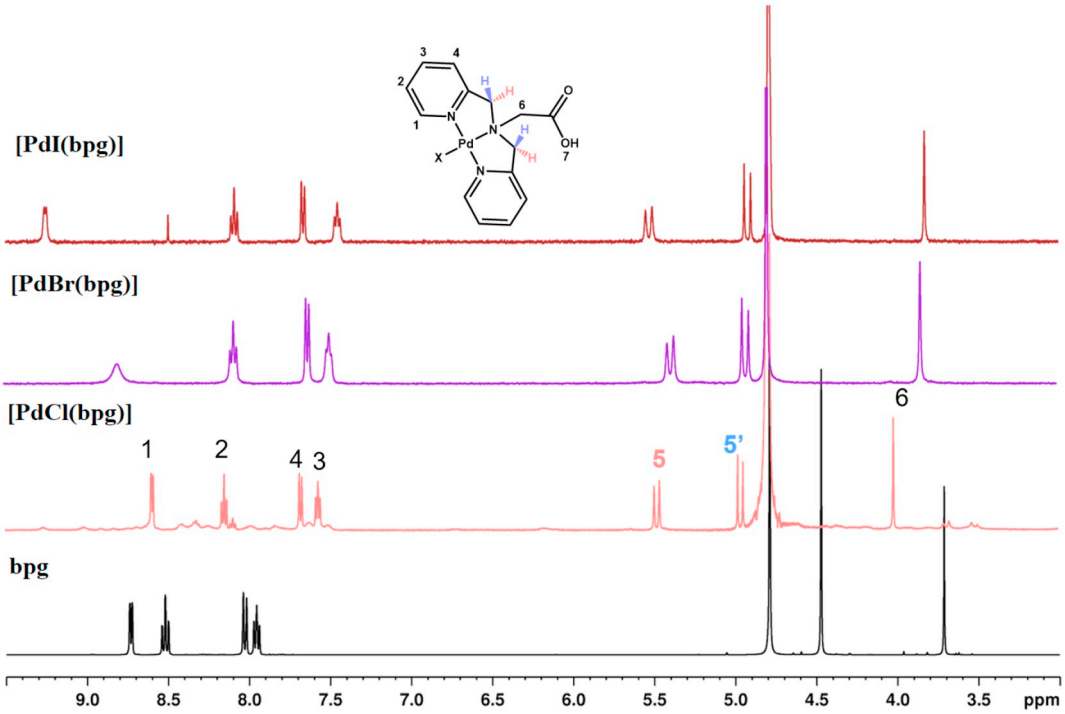

Fig. 3. ^{1}H NMR spectra of compounds bpg and [PdX(bpg)] where X = Cl, Br, I in D_2O. The ligand bpg structure with hydrogen numbering is shown for the assignment of the signals.

3.2.1. Mass spectrometry

The complexes were characterized in solution by mass spectrometry (Fig. S2). The spectrum of [PdI(bpg)] showed the molecular ion as a monocharged ion [PdI(bpg) + H^+] with monoisotopic mass 488.0187 in agreement with the calculated isotopic pattern. Similarly, the ion [PdBr(bpg) + H^+] is observed centered in *m/z* 440.0315 and [PdCl (bpg) + H^+] in *m/z* 395.9896. Interestingly, no chloride replacement is observed by mass spectrometry in the experimental conditions performed.

3.2.2. Halogen hydrolysis

As halogen hydrolysis is an important step in the mechanism of metal-based compounds, the halogen hydrolysis of [PdCl(bpg)] was further investigated. In Fig. S3 it is presented the ^{1}H NMR spectra of [PdCl(bpg)] acquired in different time points. The [PdCl(bpg)] presented exchange in D_2O solution, evidenced by the presence of lateral signals in the ^{1}H NMR spectrum acquired after 15 min of dissolution. The integrals did not change with time confirming the equilibrium was fast established in solution. After 20 h, NaCl was added to the solution and the spectrum acquired, showing a decrease of the lateral signals and a shift in the hydrogen signals. These set of data demonstrated there is an exchange of chloride ligands by water to some extent. The spectrum in the presence of KOD has no lateral signals as the basic condition forces the total exchange of the chloride ligand by hydroxide (Fig. S4). In the case of [PdBr(bpg)] and [PdI(bpg)] no exchange was observed in D_2O (Fig. 3).

3.2.3. pKa determination

The solution structure of the complexes is pH dependent, mainly because of the presence of an uncoordinated carboxylic group. The titration curve presents two inflections, one at pH 5.10 and another in pH 8.42. A distribution plot is shown in Fig. 4. One inflection represents the carboxylic deprotonation, and the pKa was determined as 4.65. As we know by NMR analysis, exchange of the chloride ligand in the complex [PdCl(bpg)] was observed. The second inflection is respective to water deprotonation as indicated in the distribution diagram and the pKa was 6.81 in agreement with the ^{1}H NMR in KOD solution.

Due to the lower solubility of [PdBr(bpg)] and [PdI(bpg)] it was not possible to acquire the pKa for these complexes.

3.3. Synthesis and characterization of Tf binding peptide-metal complex conjugate, [PdCl(bpg-TfRpep)]

The ligand bpg was designed to maintain the carboxylic acid uncoordinated after complexations reaction with a metal ion. In this work, the free carboxylic acid was used for the conjugation of a transferrin receptor binding peptide of sequence HAIYPHRH, of the monoisotopic mass of 1029.53 Da, named here TfRpep. The peptide was synthesized by Fmoc solid state automated synthesis. Subsequently, the ligand (bpg) was added in excess to the resin under TBTU activation. After cleavage of the resin, side chains deprotection and HPLC purification the bpg-TfRpep was characterized by MS showing the molecular ion monocharged in *m/z* 1269. The coordination of Pd^{II} was performed by adding $K_2[PdCl_4]$ in aqueous solution to the bpg-TfRpep, forming a pale yellow precipitate, which was collected, washed and characterized by ESI mass spectrometry. The spectrum of [PdCl(bpg-TfRpep)] showed the ions [Pd (bpg-TfRpep)]$^{2+}$ and [Pd(bpg-TfRpep) + H]$^{3+}$ with monoisotopic mass 685.7621 and 457.5201 in agreement with the calculated isotopic pattern. We also observed the likely presence of $PdCl_4$ because of fragments with *m/z* 739, 757 and 775 that were attributed to ions [Pd (bpg-TfRpep) + Pd]$^{2+}$ [Pd(bpg-TfRpep) + PdCl]$^{2+}$ and [Pd(bpg-TfRpep) + $PdCl_2$]$^{2+}$.The spectrum is shown in Fig. S5.

3.4. Antiproliferative assay

Nine tumorigenic cell lines from the National Cancer Institute 60 panel (NCI-60) were selected for the study of antiproliferative activity of the complexes [PdCl(bpg)], [PdBr(bpg)], [PdI(bpg)] and [PdCl(bpg-Tf-peptide)]. Except by renal cell adenocarcinoma (786-0) and non-tumorigenic HaCaT cell lines, all of them were reported to overexpress TfR [17]. Doxorubicin was selected as a positive control. Cisplatin was previously evaluated and reported here for comparison. The growth inhibition to achieve 50% (GI_{50}) of the compounds is reported in Table 2.

The compounds [PdI(bpg)] and [PdCl(bpg)] presented very similar antiproliferative profiles. The complex bearing iodine presented slightly lower GI_{50} values in comparison to [PdCl(bpg)] but the same trend according to the cell line. In comparison to cisplatin, the complex [PdI (bpg)] presented significantly lower GI_{50} values in the colon (HT-29), ovarian (OVCAR-3) and prostate (PC-3). Important to notice, that

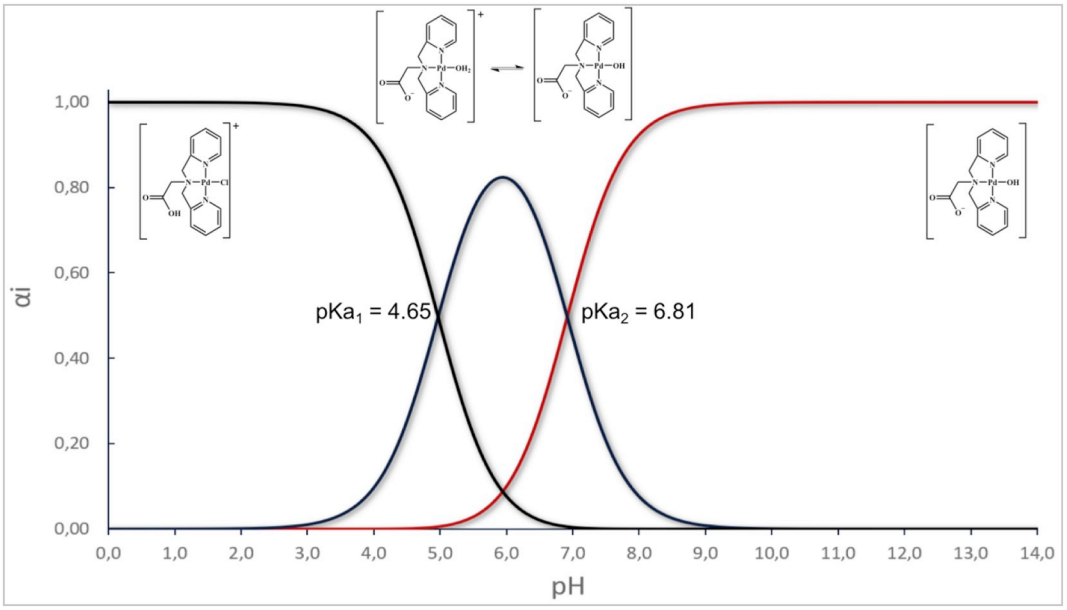

Fig. 4. Fractional composition diagram (distribution curves) for the [PdCl(bpg)] complex.

Table 2
Concentration in μM of the complexes required to promote 50% of cell proliferation inhibition (GI_{50}).

Compounds	Growth Inhibition 50% (GI_{50})									
	Cell lines[a]									
	U251	MCF-7	NCI-ADR/RES	786-O	NCI-H460	PC-3	OVCAR-03	HT-29	K562	HaCat
Doxo	0.0478	< 0.046	0.294	< 0.046	< 0.046	0.423	0.258	0.478	< 0.046	< 0.046
Cisplatin [55]	4.27	7.23	8.30	3.73	0.600	8.70	10.7	17.0	8.07	3.80
[PdI(bpg)]	5.80	6.07	5.47	5.17	15.0	5.58	6.52	7.05	0.858	12.6
[PdBr(bpg)]	32.0	39.0	45.3	44.9	31.7	49.8	43.6	46.7	37.2	31.4
[PdCl(bpg)]	6.76	8.29	4.87	6.93	13.7	7.31	7.11	28.6	3.16	11.6
[PdCl(bpg-TfRpep)[b]	196	196	196	196	83.2	196	196	196	196	196

[a] Tumorigenic human cell lines: U251 (glioblastoma), MCF-7 (breast), NCI-ADR/RES (resistant ovarium), 786–0(renal cell adenocarcinoma), NCI-H460 (Non-small lung), PC-3 (prostate), OVCAR-03 (ovarian), HT-29 (colon), K562 (leukemia). Non-tumorigenic human cell line: HaCaT (keratinocyte).
[b] Values might be overestimated.

neither chloride analog nor cisplatin had high activity at HT-29 (colon) cell line, which shows that our iodide complex does not have cross-resistance with cisplatin. In terms of selectivity [PdI(bpg)] showed the highest selectivity index in comparison to the other compounds evaluated for the K562 leukemia cells, however, analysis of the anti-proliferative curves (Fig. S6) shows that [PdI(bpg)] does not increase its cytotoxicity with concentration presenting abrupt decrease of cell viability in higher concentrations. On the other hand, [PdCl(bpg)] presents cytotoxicity directly proportional to the concentration, which suggests a more selective behavior than [PdI(bpg)]. The selectivity index of the other compounds is not significant. Changes in the monodentate ligand (halogen) can modify the cellular uptake and accumulation pathways involved in the first stages of drug action. This leads to variations in the cellular distribution of the drug and, in turn, to different apoptotic pathways being triggered because of cellular compartmentalization, hence determining differences in IC_{50} values [41,44].

The conjugation of TfR-pep to the [PdCl(bpg)] increased the GI_{50} to higher levels (no activity) and the selectivity was not improved. Previous studies show that some extent of increase in inhibitory (IC_{50}) and growth concentrations (GI_{50}) after conjugation. Lipard and co-workers observed a ten times increase in the inhibitory concentration of $[Pt^{IV}Cl_2(NH_3)_2$(succinate)(suc-CTX)] in comparison to cisplatin. On the other hand, the conjugation of RGD and NGR peptides rendered selective recognition to malignant cells by binding αvβ3 and αvβ5 integrins to the cells expressing aminopeptidase-N [6,60]. The conjugation of receptor-binding peptides, octreotide, and RGD, to ruthenium and platinum photoactivated compounds caused a decrease in the cytotoxic activity compared to its parent complexes, however, presented selective phototoxicity in the SK-MEL-28 melanoma cancer cells over-expressing the desired receptor [9,61,62]. The conjugation of the Os^{II} arene anticancer complex to cell penetrating peptides did not improve the cytotoxic activity of the parent metal complex in cancer cells, but it significantly enhanced its cellular uptake and DNA binding [63,64]. As we can see in the examples cited it is not necessarily expected an improved in the values of IC_{50} and GI_{50} by conjugation, though it is expected an improvement in the selectivity of the complexes.

In the case of [PdCl(bpg-TfR-pep)] values were too high, and the selectivity index is not significant. The hypotheses for this behavior are i) insolubility causing precipitation in the culture medium ii) hydrolysis of the peptide in the culture medium, and iii) the effect of the free carboxylic acid increase the antiproliferative activity. The insolubility in the culture medium can be observed in the antiproliferative curves (Fig. S6). The decrease of cell viability in the lower concentrations followed by an increase in the higher concentrations suggest insolubility of the compound in the culture media. The hydrolysis was also evaluated and is reported in the next section, however, no significant hydrolysis was detected. Therefore, the precipitation is the most probable hypothesis the GI_{50} values might be overestimated.

3.5. Peptide hydrolysis of [PdCl(bpg-TfRpep)]

The hydrolysis of the peptide in solution was qualitatively evaluated by mass spectrometry after incubation of the complex [PdCl(bpg-TfRpep)] in water for 24 h and 48 h at 37 °C. After 24 h we observed the appearance of a monocharged signal at *m/z* 1080 and the double charged at *m/z* 540 representing the hydrolysis of two terminal amino acids, histidine, and arginine (Fig. S7). This signal is not observed in the spectrum of [PdCl(bpg-TfRpep)] at immediate acquisition after dissolution. After 48 h the relative abundance of this signal increased significantly. The signal at *m/z* 399 representing [PdCl(bpg)] is observed with a very low relative abundance in the initial spectrum (time zero) and not a significative increase is observed after 48 h. The signals observed for [PdCl(bpg-TfRpep)] previously discussed is observed without significative changes. This analysis allows us to say that the hydrolysis is not a significative effect and the conjugate is stable in aqueous solution.

3.6. DNA interaction

The interaction with DNA of the complex [PdCl(bpg)] was evaluated by spectroscopic titration with CT-DNA according to classical methods [65,66] and electrophoretic mobility of pGEX-4T1 plasmid [67,68]. The first technique can monitor variation in the double helix structure. Hypochromism can be intercalation or electrostatic interaction. The extent of hypochromism is commonly consistent with the strength of intercalative interaction and is quantitatively determined by an intrinsic binding constant (Kb). [66,68,69] Hyperchromism is related to breaks of the secondary structure and is usually confirmed by the electrophoretic mobility, which is very sensitive to strand breaks. The pGEX-4T1 plasmid presents three forms with very distinct electrophoretic mobility on an agarose gel. The slower migration is observed for the relaxed circular form (RCF), followed by partial supercoiled (SCP) and then supercoiled form (SCF), which is the fastest.

Fig. 5 shows the results of DNA interaction in both, spectroscopic (Fig. 5a) and the electrophoretic mobility (Fig. 5b) methodologies. The Kb was determined by the Eq. (1)

$$[DNA]/(\varepsilon_a - \varepsilon_f) = [DNA]/(\varepsilon_b - \varepsilon_f) + 1/K_b(\varepsilon_b - \varepsilon_f) \quad (1)$$

where [DNA] is the concentration of CT-DNA in base pairs, ε_a is the apparent extinction coefficient obtained by calculating A_{obs}/[complex], ε_f corresponds to extinction coefficient of the complex in the free form, and ε_b refers to the extinction coefficient in the bound form.

The results show no significant complex interaction with DNA. The Kb is lower than the usual Kb for intercalative interactions, usually in

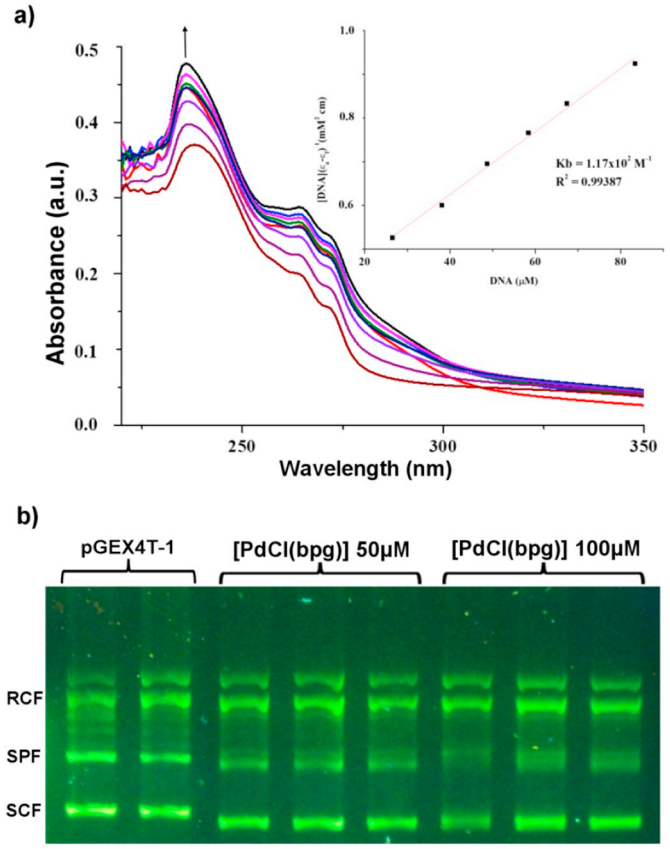

Fig. 5. a) Electronic absorption spectra of the complex [PdCl(bpg)] in the absence and presence of increasing amounts of CT-DNA. Arrows show the change in the absorbance with respect to an increase in the DNA concentration (inset: Plot of [DNA] *vs* [DNA]/(εa – εf) at 265 nm), b) Agarose gel showing the electrophoretic mobility of PGEX-4 T1 DNA plasmid with two concentrations of [PdCl(bpg)].

Table 3
BSA apparent binding constant (Kb), number of sites (n) and linear correlation coefficient of the interaction of BSA and the compounds.

Compound	K_b ($M^{-1} \times 10^3$)	n	R^2
Bpg	0.536	0.814	0.9599
[PdCl(bpg)]	1140	1.392	0.9952
[PdBr(bpg)]	9.200	1.056	0.9956
[PdI(bpg)]	1280	1.443	0.9996
[PdCl(bpg-TrfR-pep)]	5.700	1.068	0.9973

the order of $10^5\,M^{-1}$ [66,70,71]. No shifts were observed in the band, suggesting that the interaction is not significant. Electrophoretic mobility assay showed that the complex is not able to cleave the DNA, confirming that the DNA is not a target for these complexes.

3.7. BSA interaction

Human serum albumin (HSA) is the most abundant protein in the blood plasma, acts as a carrier of molecules in the organism and plays important role in the delivery of many pharmaceuticals to the sites of disease [72]. It has been reported to be essential in the transport of metallodrugs that usually occurs through a ligand exchange reaction with cysteine-34, changing the structure of HSA and the structure of the compound delivered. The Bovine Serum Albumin (BSA) is mostly used in analyses due to the high structural homology to HSA. In addition, BSA has two tryptophan residues, Trp-134 and Trp-212, whereas HSA has a single tryptophan at position 214 [73]. The tryptophan confer to BSA a strong fluorescence emission in solution at $\lambda_{em,max}$ = 352 nm, with λ_{ext} = 295 nm. Interaction of compounds with BSA produces a fluorescence quenching due to conformational changes [74]. The fluorescence emission spectra of BSA with different stoichiometric ratios of compounds were acquired (Fig. S8). The quenching was treated by Stern-Volmer equations [75,76]. The values of the association constant, apparent binding constant and number of interaction sites are reported in Table 3.

The compounds present significant different binding constants to BSA. The highest values were found for [PdI(bpg)] and [PdCl(bpg)], around 10^6, unexpectedly, [PdBr(bpg)] and the conjugate complex [PdCl(bpg-TfRpep)] presented values around 10^4 and 5×10^3 respectively, usually the large size of a drug molecule may have larger hydrophobic area which can interact with hydrophobic surface on the protein molecule, so it was expected to observe an increasing binding constant in the order [PdCl(bpg)] < [PdBr(bpg)] < [PdI (bpg)] < [PdCl(bpg-TrfR-pep)] [77]. The ligand bpg presented no significate interaction with K of order 10^2. The constants found are in the same range reported for other metal compounds [76,78–80] and are optimal as they are high enough ($> 10^3$) to bind BSA and sufficiently low ($< 10^{15}$) to be released. The number of sites follows the same trend with [PdI(bpg)] and [PdCl(bpg)] with a non-integer number around 1.5 while the other present one single site of interaction. This trend is similar to the cytotoxicity, [PdI(bpg)] and [PdCl(bpg)] presented the lowest GI_{50}. It is important to highlight that BSA can also be a good model for the interaction with sulfur-rich proteins, which can be a biomolecular target for the complexes. Hence, we can hypothesize the antiproliferative activity could be associated with the interaction with proteins and not with the DNA as expected for square planar compounds.

The competition between GSH and BSA and *N*-acetyl-cysteine and BSA showed the complex [PdCl(bpg)] is not released from BSA by these molecules in solution.

4. Conclusions

This work represents the first report on the preparation of Pd^{II} metallopeptides. The obtained conjugated [PdCl(bpg-TfR-pep)] showed high stability in diluted aqueous solution, however, it presents a lower aqueous solubility when compared to the parent complex. This lower solubility seems to be the cause for the very low cytotoxic activity observed for this conjugated complex in nine tumorigenic and non-tumorigenic cell lines evaluated. The main evidence is the increase of cell viability in higher concentrations of the compound. The free carboxylic group seems to confer the solubility needed for the activity. Interestingly and an intriguing trend was observed for the complexes coordinated to different halogens. The chloride and iodine compounds were cytotoxic while the bromine parent compound was not active. From the cytotoxicity studies, we highlight the comparative results of [PdCl(bpg)], [PdI(bpg)] and cisplatin in the cisplatin-resistant HT-29 cell line. The GI_{50} values were 28, 7 and 17 μM respectively, demonstrating the [PdI(bpg)] has not cross-resistance with cisplatin. The trend observed in the GI_{50} of [PdCl(bpg)], [PdBr(bpg)] and [PdI(bpg)] was observed for the BSA binding constant. In aqueous solution [PdCl(bpg)] readily exchange chloride while iodine and bromine do not show exchange in the evaluations performed. Therefore, the DNA binding was evaluated for the chloride compound and no interaction was observed. The evaluations suggest that DNA is not a target and sulfur-rich proteins are targets instead. The differences observed among the series with different halogens and technique to circumvent the lower solubility of the conjugate complex [PdCl(bpg-TfR-pep)] is a subject for future investigations.

Abbreviations

bpa	*N*,*N*-bis(2-picolyl)amine
bpg	bis-(2-pyridylmethyl)glycine
BSA	Bovine serum albumin
CT-DNA	Calf Thymus DNA
dien	Diethylenetriamine
Doxo	Doxorubicin
dpa	2,2'-dipicolylamine
GSH	Glutathione
HSA	Human serum albumin
terpy	Terpyridine
TBTU	O-(benzotriazol-1-yl)-N,N,N',N'-Tetramethyluronium tetrafluoroborate
tpa	tris-(2-pyridylmethyl)amine
TfR	Transferrin Receptor

Acknowledgments

We would like to thank Professor Ana Maria Ferreira da Costa for the elemental analysis. This work was financially supported by São Paulo Research Foundation (FAPESP) processes 2016/07729-4, 2017/12719-0 and 2018/13588-0 and National Council for Scientific and Technological Development (CNPq) grant no. 140384/2016-2 and 406444/2018-8 and partially supported by Coordenação de Aperfeiçoamento de Pessoal de Nível Superior - Brasil (CAPES) - Finance Code 001.

Appendix A. Supplementary data

Supplementary data to this article can be found online at https://doi.org/10.1016/j.jinorgbio.2019.110754.

References

[1] I. Romero-Canelon, P.J. Sadler, Inorg. Chem. 52 (2013) 12276–12291.
[2] K.L. Haas, K.J. Franz, Chem. Rev. 109 (2009) 4921–4960.
[3] C. Alvarez-Lorenzo, A. Concheiro, Chem. Commun. 50 (2014) 7743–7765.
[4] C. Dolan, C.S. Burke, A. Byrne, T.E. Keyes, K.K.-W. Lo (Ed.), Inorganic and Organometallic Transition Metal Complexes with Biological Molecules and Living Cells, Academic Press, 2017.
[5] M. Soler, L. Feliu, M. Planas, X. Ribas, M. Costas, Dalton Trans. 45 (2016) 12970–12982.
[6] S. Mukhopadhyay, C.M. Barnés, A. Haskel, S.M. Short, K.R. Barnes, S.J. Lippard, Bioconjug. Chem. 19 (2008) 39–49.
[7] S.H.v. Rijt, H. Kostrhunova, V. Brabec, P.J. Sadler, Bioconjug. Chem. 22 (2011) 218–226.
[8] A. Leonidova, V. Pierroz, R. Rubbiani, J. Heier, S. Ferrari, G. Gasser, Dalton Trans. 43 (2014) 4287–4294.
[9] F. Barragán, P. López-Senín, L. Salassa, S. Betanzos-Lara, A. Habtemariam, V. Moreno, P.J. Sadler, V. Marchán, J. Am. Chem. Soc. 133 (2011) 14098–14108.
[10] L. Blackmore, R. Moriarty, C. Dolan, K. Adamson, R.J. Forster, M. Devocelle, T.E. Keyes, Chem. Commun. 49 (2013) 2658–2660.
[11] F. Noor, R. Kinscherf, G.A. Bonaterra, S. Walczak, S. Wölfl, N. Metzler-Nolte, ChemBioChem 10 (2009) 493–502.
[12] F. Noor, A. Wüstholz, R. Kinscherf, N. Metzler-Nolte, Angew. Chem. Int. Ed. 44 (2005) 2429–2432.
[13] M. Kawamoto, T. Horibe, M. Kohno, K. Kawakami, BMC Cancer 11 (2011) 359–371.
[14] M.G. Mendoza-Ferri, C.G. Hartinger, M.A. Mendoza, M. Groessl, A.E. Egger, R.E. Eichinger, J.B. Mangrum, N.P. Farrell, M. Maruszak, P.J. Bednarski, F. Klein, M.A. Jakupec, A.A. Nazarov, K. Severin, B.K. Keppler, J. Med. Chem. 52 (2009) 916–925.
[15] C. Wängler, D. Nada, G. Höfner, S. Maschauer, B. Wängler, S. Schneider, E. Schirrmacher, K.T. Wanner, R. Schirrmacher, O. Prante, Mol. Imaging Biol. 13 (2011) 332–341.
[16] P. Youn, Y. Chen, D.Y. Furgeson, Mol. Pharm. 11 (2014) 486–495.
[17] T.R. Daniels, E. Bernabeu, J.A. Rodríguez, S. Patel, M. Kozman, D.A. Chiappetta, E. Holler, J.Y. Ljubimova, G. Helguera, M.L. Penichet, Biochim. Biophys. Acta Gen. Subj. 1820 (2012) 291–317.
[18] T.R. Daniels, T. Delgado, G. Helguera, M.L. Penichet, Clin. Immunol. 121 (2006) 159–176.
[19] S. Kasibhatla, K.A. Jessen, S. Maliartchouk, J.Y. Wang, N.M. English, J. Drewe, L. Qiu, S.P. Archer, A.E. Ponce, N. Sirisoma, S. Jiang, H.-Z. Zhang, K.R. Gehlsen, S.X. Cai, D.R. Green, B. Tseng, Proc. Natl. Acad. Sci. U. S. A. 102 (2005) 12095–12100.
[20] Y. Wu, J. Xu, J. Chen, M. Zou, A. Rusidanmu, R. Yang, Thoracic Cancer 9 (2017) 253–261.
[21] I. Artuso, M.R. Lidonnici, S. Altamura, G. Mandelli, M. Pettinato, M.U. Muckenthaler, L. Silvestri, G. Ferrari, C. Camaschella, A. Nai, Blood (2018) 2286–2297.
[22] M. Singh, H. Atwal, R. Micetich, Anticancer Res. 18 (1998) 1423–1427.
[23] T. Hoshino, M. Misaki, M. Yamamoto, H. Shimizu, Y. Ogawa, H. Toguchi, J. Pharm. Sci. 84 (1995) 216–221.
[24] J.H. Lee, J.A. Engler, J.F. Collawn, B.A. Moore, Eur. J. Biochem. 268 (2001) 2004–2012.
[25] S. Oh, B.J. Kim, N.P. Singh, H. Lai, T. Sasaki, Cancer Lett. 274 (2009) 33–39.
[26] D.R. van Staveren, N. Metzler-Nolte, Chem. Commun. (2002) 1406–1407.
[27] B. Albada, N. Metzler-Nolte, Chem. Rev. 116 (2016) 11797.
[28] M.S. Robillard, A.R.P.M. Valentijn, N.J. Meeuwenoord, G.A. van der Marel, J.H. van Boom, J. Reedijk, Angew. Chem. Int. Ed. 39 (2000) 3096–3099.
[29] J.-M. Pagès, S. Kascàkovà, L. Maigre, A. Allam, M. Alimi, J. Chevalier, E. Galardon, M. Réfrégiers, I. Artaud, ACS Med. Chem. Lett. 4 (2013) 556–559.
[30] A. Allam, L. Maigre, M. Alimi, R. Alves de Sousa, A. Hessani, E. Galardon, J.-M. Pagès, I. Artaud, Bioconjug. Chem. 25 (2014) 1811–1819.
[31] T. Lazarević, A. Rilak, Ž.D. Bugarčić, Eur. J. Med. Chem. 142 (2017) 8–31.
[32] A. Garoufis, S.K. Hadjikakou, N. Hadjiliadis, Coord. Chem. Rev. 253 (2009) 1384–1397.
[33] A.R. Khokhar, Q.Y. Xu, Z.H. Siddik, J. Inorg. Biochem. 39 (1990) 117–123.
[34] C.K. Mirabelli, D.T. Hill, L.F. Faucette, F.L. McCabe, G.R. Girard, D.B. Bryan, B.M. Sutton, J.O. Bartus, S.T. Crooke, R.K. Johnson, J. Med. Chem. 30 (1987) 2181–2190.
[35] F.L. Wimmer, S. Wimmer, P. Castan, S. Cros, N. Johnson, E. Colacio-Rodrigez, Anticancer Res. 9 (1989) 791–793.
[36] P. Castan, E. Colacio-Rodriguez, A.L. Beauchamp, S. Cros, S. Wimmer, J. Inorg. Biochem. 38 (1990) 225–239.
[37] R.G. Buckley, S.P. Fricker (Ed.), Metal Compounds in Cancer Therapy, Springer Netherlands, Dordrecht, 1994, pp. 92–108.
[38] Z. Iakovidou, A. Papageorgiou, M.A. Demertzis, E. Mioglou, D. Mourelatos, A. Kotsis, P. Nath Yadav, D. Kovala-Demertzi, Anti-Cancer Drugs 12 (2001) 65–70.
[39] E. Guney, V.T. Yilmaz, F. Ari, O. Buyukgungor, E. Ulukaya, Polyhedron 30 (2011) 114–122.
[40] G. Ayyannan, M. Mohanraj, G. Raja, N. Bhuvanesh, R. Nandhakumar, C. Jayabalakrishnan, Inorg. Chim. Acta 453 (2016) 562–573.
[41] L. Tušek-Božić, I. Matijašić, G. Bocelli, G. Calestani, A. Furlani, V. Scarcia, A. Papaioannou, J. Chem. Soc. Dalton Trans. (1991) 195–201.
[42] M.J. Cleare, J.D. Hoeschele, Bioinorg. Chem. 2 (1973) 187–210.
[43] L. Messori, L. Cubo, C. Gabbiani, A. Álvarez-Valdés, E. Michelucci, G. Pieraccini, C. Ríos-Luci, L.G. León, J.M. Padrón, C. Navarro-Ranninger, A. Casini, A.G. Quiroga, Inorg. Chem. 51 (2012) 1717–1726.
[44] I. Romero-Canelón, L. Salassa, P.J. Sadler, J. Med. Chem. 56 (2013) 1291–1300.
[45] Y.-H. Chiu, J.W. Canary, Inorg. Chem. 42 (2003) 5107–5116.
[46] G. Sheldrick, Acta Cryst. A 71 (2015) 3–8.
[47] O.V. Dolomanov, L.J. Bourhis, R.J. Gildea, J.A.K. Howard, H. Puschmann, J. Appl. Crystallogr. 42 (2009) 339–341.
[48] G. Sheldrick, Acta Cryst. A 64 (2008) 112–122.
[49] I.G.R. Gutz. programa CurTiPot - pH e Curvas de Titulação Potenciométrica: Análise e Simulação, versão 4.2, http://www.iq.usp.br/gutz/Curtipot.html
[50] H.A. El-Asmy, I.S. Butler, Z.S. Mouhri, B.J. Jean-Claude, M. Emmam, S.I. Mostafa, Inorg. Chim. Acta 441 (2016) 20–33.
[51] R.N. Silva, L.C.G. Oliveira, C.B. Parise, J.R. Oliveira, B. Severino, A. Corvino, P. di Vaio, P.A. Temussi, G. Caliendo, V. Santagada, L. Juliano, M.A. Juliano, Biochim. Biophys. Acta 1865 (2017) 558–564.
[52] B.J. Backes, J.L. Harris, F. Leonetti, C.S. Craik, J.A. Ellman, Nat. Biotechnol. 18 (2000) 187–193.
[53] A. Monks, D. Scudiero, P. Skehan, R. Shoemaker, K. Paull, D. Vistica, C. Hose, J. Langley, P. Cronise, A. Vaigro-Wolff, M. Gray-Goodrich, H. Campbell, J. Mayo, M. Boyd, J. Natl. Cancer Inst. 83 (1991) 757–766.
[54] R.H. Shoemaker, Nat. Rev. Cancer 6 (2006) 813–823.
[55] J.H.B. Nunes, F.R.G. Bergamini, W.R. Lustri, P.P. de Paiva, A.L.T.G. Ruiz, J.E. de Carvalho, P.P. Corbi, J. Fluor. Chem. 195 (2017) 93–101.
[56] P.J. Sanz Miguel, P. Lax, B. Lippert, J. Inorg. Biochem. 100 (2006) 980–991.
[57] R. Melanson, J. Hubert, F.D. Rochon, Can. J. Chem. 53 (1975) 1139–1143.
[58] F.D. Rochon, P.C. Kong, B. Coulombe, R. Melanson, Can. J. Chem. 58 (1980) 381–386.
[59] S. Coşar, M.B.L. Janik, M. Flock, E. Freisinger, E. Farkas, B. Lippert, J. Chem. Soc., Dalton Trans. (1999) 2329–2336.
[60] T.C. Johnstone, K. Suntharalingam, S.J. Lippard, Chem. Rev. 116 (2016) 3436–3486.
[61] A. Gandioso, E. Shaili, A. Massaguer, G. Artigas, A. González-Cantó, J.A. Woods, P.J. Sadler, V. Marchán, Chem. Commun. 51 (2015) 9169–9172.
[62] F. Barragán, D. Carrion-Salip, I. Gómez-Pinto, A. González-Cantó, P.J. Sadler, R. de Llorens, V. Moreno, C. González, A. Massaguer, V. Marchán, Bioconjug. Chem. 23 (2012) 1838–1855.
[63] S.H. van Rijt, A.J. Hebden, T. Amaresekera, R.J. Deeth, G.J. Clarkson, S. Parsons, P.C. McGowan, P.J. Sadler, J. Med. Chem. 52 (2009) 7753–7764.
[64] A.K. Renfrew, A.D. Phillips, A.E. Egger, C.G. Hartinger, S.S. Bosquain, A.A. Nazarov, B.K. Keppler, L. Gonsalvi, M. Peruzzini, P.J. Dyson, Organometallics 28 (2009) 1165–1172.
[65] A.R. Peacocke, J.N.H. Skerrett, Trans. Faraday Soc. 52 (1956) 261–279.
[66] Parsekar, S.U., Fernandes, J., Banerjee, A. et al. J Biol Inorg Chem 23 (2018) 1331–1349.
[67] S.Q. Gomes, L. Vitoriano, E.G.R. de Arruda, A.L.T.G. Ruiz, T. Candido, J.E. de Carvalho, W.R. Lustri, C. Abbehausen, J. Inorg. Biochem. 186 (2018) 104–115.
[68] N. Shahabadi, S. Kashanian, M. Mahdavi, S. Noorkaram, Bioinorg. Chem. Appl. 2011 (2011).
[69] M.J. Waring, J. Mol. Biol. 13 (1965) 269–282.
[70] A. Wolfe, G.H. Shimer, T. Meehan, Biochemistry 26 (1987) 6392–6396.

[71] J.K. Barton, A. Danishefsky, J. Goldberg, J. Am. Chem. Soc. 106 (1984) 2172–2176.
[72] E.-j. Gao, L. Wang, M.-c. Zhu, L. Liu, W.-z. Zhang, Eur. J. Med. Chem. 45 (2010) 311–316.
[73] X.M. He, D.C. Carter, Nature 358 (1992) 209–215.
[74] J. Steinhardt, J. Krijn, J.G. Leidy, Biochemistry 10 (1971) 4005–4015.
[75] Y.V. Il'ichev, J.L. Perry, J.D. Simon, J. Phys, Chem. B 106 (2002) 452–459.
[76] J.R. Lacowicz, S.S. Media (Ed.), Book Principles of Fluorescence Spectroscopy, Springer US, New York, 2006.
[77] C. Abbehausen, C.M. Manzano, P.P. Corbi, N.P. Farrell, J. Inorg. Biochem. 165 (2016) 136–145.
[78] X. Yu, Y. Yang, L. Shiyu, Q. Yao, L. Heting, L. Xiaofang, Y. Pinggui, Spectrochim. Acta A Mol. Biomol. Spectrosc. 83 (2011) 322–328.
[79] K. Karami, Z.M. Lighvan, S.A. Barzani, A.Y. Faal, M. Poshteh-Shirani, T. Khayamian, V. Eigner, M. Dušek, New J. Chem. 39 (2015) 8708–8719.
[80] D. Ćoćić, S. Jovanović, S. Radisavljević, J. Korzekwa, A. Scheurer, R. Puchta, D. Baskić, D. Todorović, S. Popović, S. Matić, B. Petrović, J. Inorg. Biochem. 189 (2018) 91–102.